Thermochimica Acta 513 (2011) 60–67

Contents lists available at ScienceDirect

Thermochimica Acta

journal homepage: www.elsevier.com/locate/tca

Understanding of thermo-gravimetric analysis to calculate number of addends in multifunctional hemi-ortho ester derivatives of fullerenol

Rachana Singh [a], Thakohari Goswami [b,*]

[a] Department of Chemistry, Clemson University, Clemson, SC, USA
[b] Electronics and Smart Materials Division, Defence Materials and Stores Research and Development Establishment, DMSRDE P.O., G.T. Road, Kanpur 208013, India

ARTICLE INFO

Article history:
Received 16 September 2010
Received in revised form 2 November 2010
Accepted 8 November 2010
Available online 12 November 2010

Keywords:
Fullerene derivatives
TGA
Fullerenol
Cage multiple functionalization

ABSTRACT

Test results for the applicability of existing thermo-gravimetric analysis (TGA) technique to ascertain average number of exohedral chemical attachment in a new class of fullerene dyads consisting of multiple hemi-ortho esters onto fullerenol is presented. Although the method is nicely applicable for higher fullerenol, but homogeneous phase products calculate lower number of addends, whereas, the hetero phase products indicate higher value. Lower value is attributed to either overlapping of thermal events or substituents effects and higher value is the contribution of tetra butyl ammonium hydroxide (TBAH) impurity used as phase transfer catalyst (PTC) in heterogeneous phase reactions. Presence of TBAH impurity is recognized through thermo-gravimetry mass spectrometry (TG-MS) measurement. Appropriate modification of test method to arrive at accurate and precise values of *x* (total mass contribution due to addends only) and *y* (total mass contribution due to fullerene plus char yield) are also reported. Successful use of two more different techniques, viz., electron-spray ionization mass spectrometry (ESI-MS) and X-ray photoelectron spectroscopy (XPS), supplement above results. Influences of fullerene and different substituents on thermal behavior of dyads are assessed.

1. Introduction

Exploitation of peculiar electronic properties of fullerenes for solar energy conversion has become a field of intensive investigation [1–6]. Extensive research is going on to develop methodology for covalent exohedral functionalization of fullerene attaching different types of addends [7–10]. Rapid advancement in fullerene chemistry revealed the covalent functionalization of fullerene with various donors and many fullerene based donor–acceptor dyads have been synthesized [11]. This molecular approach for solar energy conversion appeared to be particularly interesting, since the bi-continuous network obtained by chemically linking of hole-conducting donor moiety to the electron-conducting fullerene subunit prevents any problem arising from bad contacts at the junction due to phase separation, as observed for polymer/fullerene blends [12]. C_{60} is a potential electron acceptor due to its low reduction potential [13], three-dimensional structure [14] and small reorganization energy [15] and has the ability to retain its redox as well as photophysical properties after derivatization. Several types of donor molecules, mostly as mono or bis adduct have been employed so far to the C_{60}-dyad component [11]. Multi-functional fullerene derivatives have attracted very low attention in spite of having several interesting properties [16–20]. Multiple functionalizations may offer new opportunities in the search for fullerene materials that are amenable to potential technological applications. As an extreme in C_{60} cage multiple functionalizations, comparative fluorescence study of exohedrally attached 28-vinyl ester groups (hemi-ortho ester) on $C_{60}(OH)_{28}$-fullerenol is reported earlier [21].

Beside solar energy conservation and storage, fullerenols find interesting applications in many other fields, viz., fuel cells [22,23], macromolecular materials [24,25] and biomedical and life sciences as photosensitizers for photodynamic therapy (PDT) and free-radical scavengers for anti-oxidant drugs [26–30]. Studies on the biological properties of fullerenols demonstrate that they are efficient free radical (superoxide radical O_2^-) scavenger and able to reduce the concentration of free radicals in pathological blood and also inhibit the growth of abnormal and ailing cells [31,32]. Gadolinium fullerenols are reported to be the best candidate for new generation novel magnetic resonance imaging (MRI) contrast agent [33–37]. Fullerenols also have potential applications in aqueous solution chemistry, electrochemistry [38] and biochemistry [39].

Fullerenol has attracted extensive attention due to high solubility, stability and reactivity. Depending on the number of hydroxyl groups, solubility of fullerenol ranges from organic to water [40,41]. Reactivity of fullerenol arises due to strong electrophilic charac-

* Corresponding author. Fax: +91 512 2450404/2404774.
E-mail address: thgoswami@yahoo.co.uk (T. Goswami).

0040-6031/$ – see front matter © 2010 Elsevier B.V. All rights reserved.
doi:10.1016/j.tca.2010.11.012

ter of fullerene and in alkaline solution fullerenol easily releases proton(s) to generate fulleroxide nucleophile. These nucleophiles undergo several interesting reaction pathways: (1) selective nucleophilic addition reaction to the carbonyl group [21,42]; (2) Michael addition reaction with α,β-unsaturated esters [43,44]; (3) reaction with isocyanates to form polyurethane [45]; (4) nucleophilic displacement as well as trans-esterification reaction with silicon derivatives [46], etc.

Excellent selectivity of fullerenol towards nucleophilic addition reaction onto carbonyl groups of different vinyl esters (**1**–**3**) is uniquely manipulated to achieve double bond terminated vinyl hemi-ortho ester derivatives of fullerenol dyads. In the present case $C_{60}(OH)_{28}$ has been used as fullerene source and very soft-chemical condition (room temperature reaction, 25 °C) is adapted to develop these materials. Reactions have been carried out in homogeneous and heterogeneous phase using methanol as co-solvent and tetra butyl ammonium hydroxide (TBAH) as phase transfer catalyst, respectively (Scheme 1). Products are characterized by different techniques and TG-MS measurement is employed to evaluate the presence of small TBAH impurity (used as PTC in heterogeneous phase reactions).

Present article highlights the capability of simple thermogravimetric analysis (TGA) technique to ascertain exohedral chemical attachment of multiple hemi-ortho esters onto fullerenol and calculation of their average number in this new class of dyads. While applying the existing methodology [47] in the present system, it is observed that although the method is nicely applicable for higher fullerenol but homogeneous phase products calculate lower number of addends whereas the hetero phase products indicate higher value. Critical analysis of the results suggest that selection of temperature zone needs to be modified in order to avoid overlapping of thermal events and/or extended thermal events due to stability of the addends in case of homogeneous phase products. Thus, in each case, temperature zone is varied depending on the stability of the addends to get accurate value of *x* (the total mass contribution due to addends) and *y* (the total mass contribution due to fullerene plus char yield). The article illustrates how accurate values of *x* and *y* will allow to calculate exact number of addends in fullerene adducts. Significant influence of fullerene and substituent(s) on the thermal characteristics of dyads is elaborated. It is quite unique to get stable hemi-ortho esters in fullerene derivatives and stability is explained on the basis of limited conformational mobility which prevents the subsequent hydrolysis.

2. Results and discussion

2.1. Synthesis

2.1.1. Fullerenol

Fullerenol isomer [$C_{60}(OH)_{28}$] used in the present investigation, is synthesized by reported method [40]. It is observed that the same combination of reagents can produce different fullerenol isomers in suitably modified reaction condition [41].

2.1.2. Hemi-ortho ester derivatives $(VEn)_{28}$–C_{60}

Scheme 1 describes the synthesis of acyclic hemi ortho-ester addended fullerenol derivatives. In a typical synthesis, conc. NaOH solution is added to an aqueous solution of fullerenol and stirred for 30 min to generate fulleroxide anions. Dilute methanolic solution of vinyl ester (1–3, 10 eq. per hydroxyl group) is then added very slowly to the ice-cooled alkaline fullerenol solution under inert atmosphere over an hour with constant stirring. Temperature is slowly raised to room temperature (25 °C) and stirring is continued for 24 h. Progress of the reaction is monitored by thin layer chromatography (TLC). Crude products $(VEn)_{28}$–C_{60} (*n* = 1a–3a) precipitate is extracted with dichloromethane and finally purified by column chromatography [mixed solvents; toluene:dichloromethane = 80:20]. In a similar manner, heterogeneous phase reaction [$(VE2b)_{28}$–C_{60}] is carried out by direct addition of vinyl ester (vinyl acetate) to the alkaline aqueous solution of fullerenol at room temperature in presence of tetrabutyl ammonium hydroxide (TBAH) as phase transfer catalyst. Above mentioned work-up procedure is also followed in this case. In comparison to heterogeneous phase reaction, homogeneous phase reaction proceeds smoothly with good reproducible result in terms of yield and product purity. Attachment of multiple aliphatic addends considerably improves the solubility and processability of fullerene. These brick-red free standing solid powdered hemi-ortho esters $(VEn)_{28}$–C_{60} (n = 1a–3a and 2b) are highly soluble in all common organic solvents and have excellent coating property.

2.2. Stability of hemi-ortho ester

"Tetrahedral" or addition–elimination mechanism (generally a second-order mechanism) most often proceeds by initial nucleophilic attack on triagonal carbonyl carbon giving a tetrahedral intermediate containing both nucleophile and leaving group. Hemi-ortho ester derivatives can be viewed as a tetrahedral intermediate formed by selective nucleophilic addition of fullerenol to the carbonyl carbon of vinyl ester. Stereo-electronic control affecting the elimination step in tetrahedral intermediate depends on the conformational mobility of the intermediate, more specifically, the position of the lone pairs, which should be anti-periplanar to the leaving group (anti-periplanar lone pair hypothesis). In some cases, tetrahedral intermediates have been isolated [48,49] or detected spectroscopically due to conformational immobility of the intermediate [50–53]. These ortho-esters are extremely resistant to hydrolysis by base but easily hydrolyzed by dilute acids due to the formation of carbocations of type $(RO)_3$–C^+ that are greatly stabilized by resonance.

Fullerenol, which generate $(Fol)^{n-}$ anion under basic condition, undergo selective nucleophilic addition reaction to the carbonyl carbon of the vinyl esters to form hemi-ortho ester via tetrahedral mechanism. The stability of the hemi-ortho ester under basic condition (as discussed earlier) arises due to strong hydrogen bonding among hemiketal –OH groups and also with residual OH groups of unreacted fullerenol. Hydrogen bonding limits the conformational mobility to prevent the second step in tetrahedral mechanism or hydrolysis to occur. It is believed that strong electronic interactions due to close proximity, geometrical orientation and stereo-electronic interaction of the flexible ether linked vinylic double bonds also contribute to stabilize the hemi ortho-ester structure.

2.3. Estimation of number of addends per fullerene

Number of hydroxyl groups in water soluble fullerenol and hemi-ortho ester units in dyads is estimated by electro-spray ionization mass spectrometry (ESI-MS), X-ray photoelectron spectroscopy (XPS) and thermo gravimetrical analysis (TGA).

2.3.1. Electro-spray ionization mass spectrometry (ESI-MS)

2.3.1.1. $C_{60}(OH)_{28}$. ESI-MS recorded in water shows molecular ion peak at *m*/*z* 1196 (M+) corresponding to 28-hydroxyl groups (supporting information).

2.3.1.2. $(VEn)_{28}$–C_{60}. Mass spectrum of $(VE1a)_{28}$–C_{60} recorded in methanol shows molecular ion peak at *m*/*z* 3980 corresponds to the attachment of 28 units onto single fullerene core (Fig. 1). Most abundant and stable ion at *m*/*z* 3880 (corresponding to 27 units)

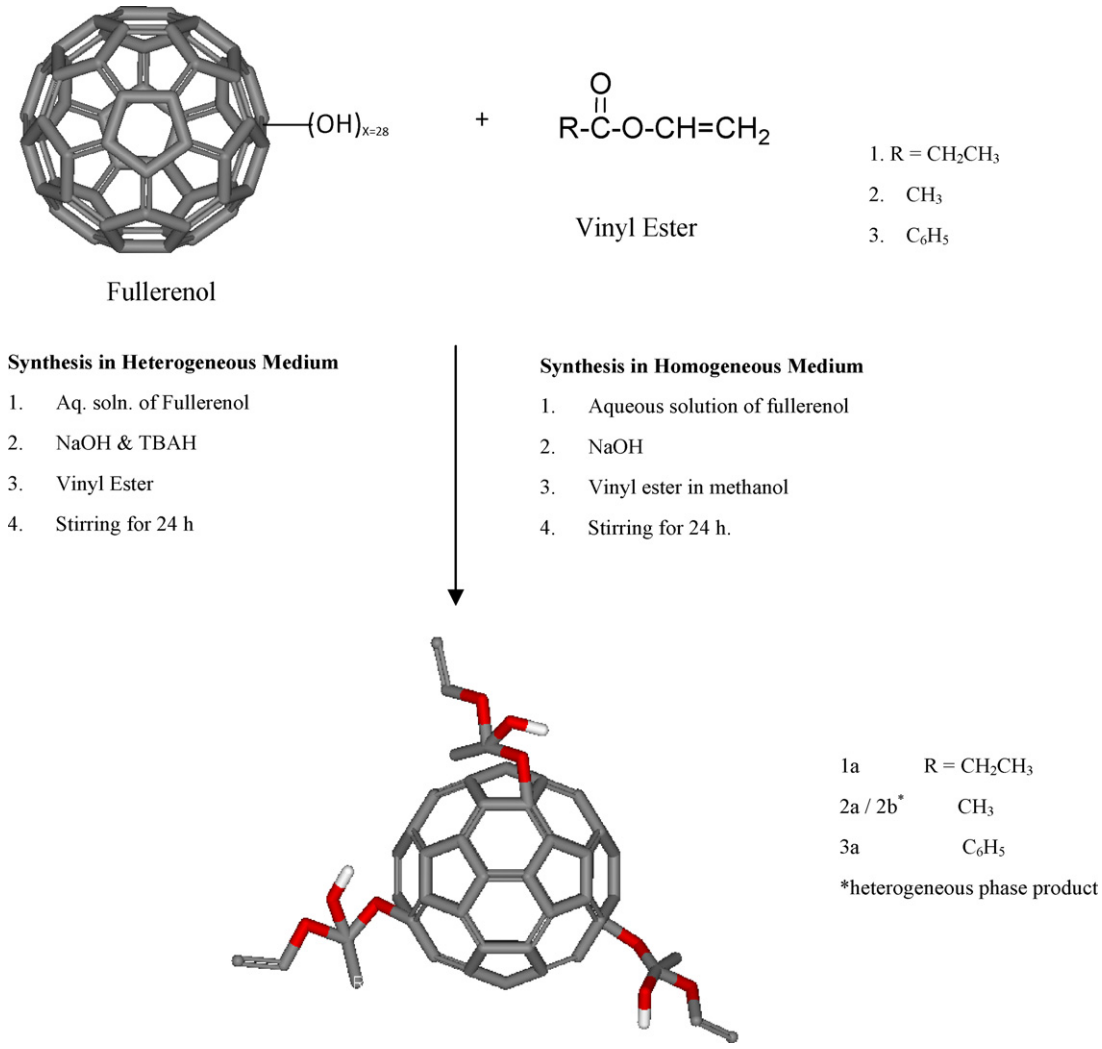

Scheme 1. Schematic representation for the formation of double bond terminated fullerene core star-like hemi-ortho esters (1a–3a and 2b) by the reaction of fullerenol with vinyl esters (1–3) in homogeneous and heterogeneous conditions. 28-vinyl ester groups are attched per fullerene. For clarity reason only three groups are shown.

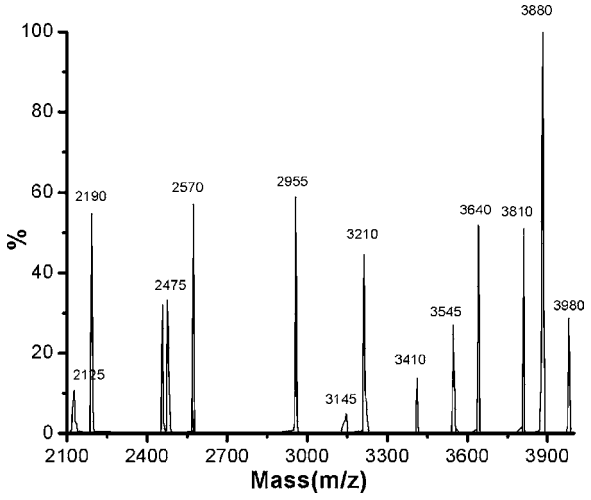

Fig. 1. ESI-MS spectrum of $(VE1a)_{28}$–C_{60} recorded in methanol.

is assigned as base peak. Assignment of other significant peaks is presented in Section 4.

2.3.2. X-ray photoelectron spectroscopy (XPS)

2.3.2.1. $C_{60}(OH)_{28}$. Electron spectroscopy for chemical analysis (ESCA) is obtained by X-ray photoelectron spectrometer equipped with a monochromatic X-ray source. ESCA analysis is performed at a nominal photoelectron take off angle of 45° and the depth of analysis for these samples is 100 Å. Relative atomic% of each element at the surface is estimated from the peak areas using atomic sensitivity factors specified for the spectrometer. Number of hydroxyl groups is also calculated by XPS. XPS of fullerenol (C 1s binding energies spreading over 5.3 eV) clearly deviates from the C 1s peak of fullerene (Fig. 2A). Large shift indicates a relatively higher percentage of higher oxidation state carbon in fullerenol compared to fullerene [54]. Large shift of C 1s binding energy and also higher than the normal C 1s binding energy of hydrocarbons (285.5 than 285 eV) reveals the functionalization of the fullerene ball. Curve-fitting analysis of fullerenol samples show two more different oxidation states of carbons allowing the assignment of three different oxidation states of carbon; sp^2 non-functionalized carbons assigned at 285.5 eV, mono-functionalized (C–OH) carbons centered at 286.8 eV and dioxygenated [carbonyl (C=O)/ketal (RO–C–OR)/hemi-ketal (RO–C–OH)] carbons at 288.9 eV. Since no carbonyl absorption peak is observed in the IR spectrum of

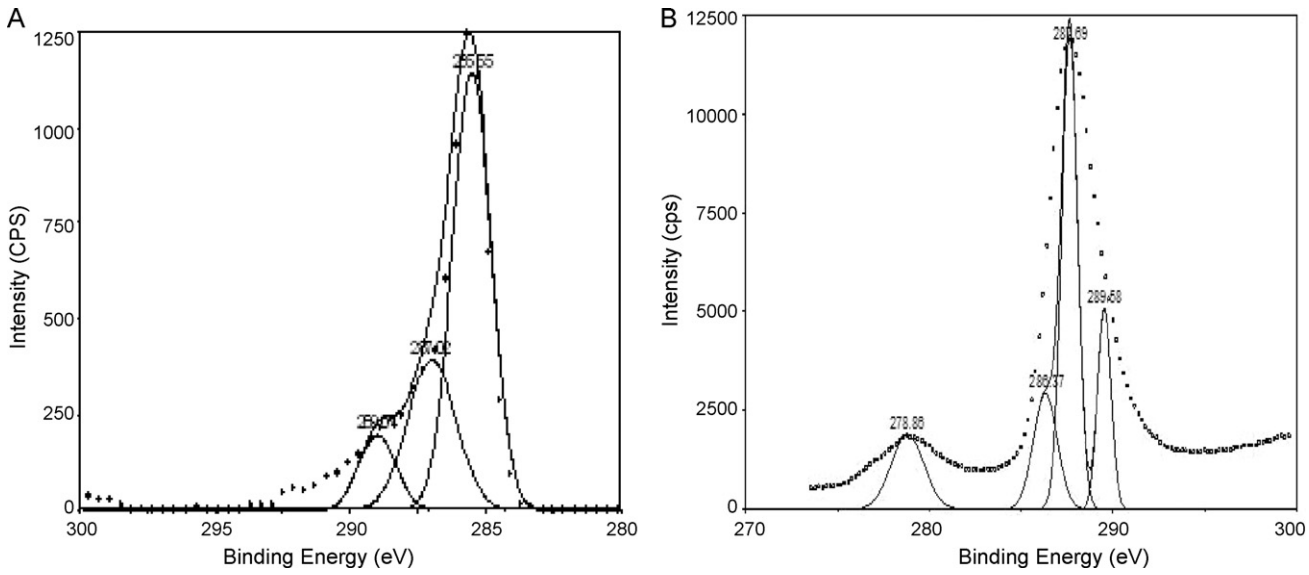

Fig. 2. XPS of (A) $C_{60}(OH)_{28}$ and (B) $(VE2a)_{28}$–C_{60}.

Table 1
Calculation of the number of addends by XPS: (A) hydroxyl groups in $C_{60}(OH)_{28}$ and (B) hemi-ortho ester units in $(VE2a)_{28}$–C_{60}.

Peak	Area	Center	% Area	No./type of Carbon
(A)				
1	1491.41	285.54	45.9	27.58/sp^2
2	1556.87	286.87	47.9	28.8/C–OH
3	197.214	288.95	6.07	3.6/dioxygenated
(B)				
4	4218	278.8	15.75	27.09/CH_3
5	4726	286.3	17.65	30.36/C–O–
6	13120	287.6	49.02	84.33/sp^2
7	4700	289.5	17.56	30.2/dioxygenated

fullerenol, the highest oxidation state is attributed to hemi-ketal carbon. Percentage area covered under each oxidation state is in the ratio of 46:48:6 and accordingly the number of different oxidation states of carbon exist in the ratio of 46:48:6 (Table 1A). As fullerene contains sixty carbons in its pristine structure, calculation from the above ratio estimate an average of 28 mono-oxygenated carbons (28 hydroxyl groups) per fullerene.

2.3.2.2. $(VEn)_{28}$–C_{60}. Number of addends in the product is also calculated by XPS. Curve fitting analysis of $(VE2a)_{28}$–C_{60} (Fig. 2B) shows four peaks representing four different oxidation states of carbon in product compared to three in fullerenol. Lowest energy oxidation state carbon peak at 278.8 eV is assigned to methyl groups present in vinyl acetate chain. Mono-functional carbons (C–OH) and sp^2 hybridized carbons are centered at 286.3 and 287.6 eV, respectively. Tri-oxigenated hemi-ortho ester carbon peak is observed at 289.5 eV. Calculation of number of carbon atoms per peak (Table 1B) gives quantitative prediction for the attachment of 28 addends. Increase in tri-oxygenated carbons number compared to fullerenol support hemi-ortho ester structure. Many folds increased in number of sp^2-hybridized carbons are due to attach vinylic groups and experimental value agrees for the presence of 28 vinylic bonds (56 sp^2-vinylic carbons + 28 in fullerenol = 84). Twenty-seven methyl groups are calculated from XPS data. XPS calculation thus establishes hemi-ortho ester structure having 28-vinyl units exohedrally attached per fullerene ball.

2.3.3. Thermo gravimetrical analysis (TGA)

Versatility of early reported thermal analysis technique is extrapolated to calculate the number of hydroxyl (addends) groups attached on fullerene moiety in present cases [47]. Assuming percentage weight loss in temperature range of 150–570 °C corresponds to the removal of all addends per fullerene = x and percentage weight loss above 570 °C corresponds to the structural degradation of fullerene plus char yield is due to fullerene only = y.

Then number of groups attached per fullerene is given by $\frac{720}{y} \times \frac{x}{M}$ (1)

where M is the weight of each group attached, e.g., $M = 17$ for –OH group. Calculating x and y from TGA thermogram, one can easily calculate the number of groups attached per fullerene from Eq. (1). Now, if M is the molecular mass of the addend reacted with fullerenol, and then $M/17$ is the hydroxyl group equivalent per added group. For example, $M = 89$ for vinyl ethanoate (1a), then 89/17 = 5 hydroxyl groups are equivalent to one vinyl ethanoate.

2.3.3.1. $C_{60}(OH)_{28}$. Following TGA and first derivative TGA trace of fullerenol, percentage weight loss between temperature range 150–570 °C is found to be 35% and the structural degradation of fullerene plus char yield contributes 52%. Then, the number of –OH groups attached per fullerene is calculated using Eq. (1) will be:

$$\frac{720}{52} \times \frac{35}{17} = 28.5$$

This nicely matches with other results.

2.3.3.2. $(VEn)_{28}$–C_{60}. Percentage weight loss obtained from TGA trace of the product between temperature range of 150–570 °C is used to calculate the number of substituents attached per fullerene in case of hemi-ortho esters. Calculating total percentage weight loss of the products in terms of addends units between temperature ranges of 150 and 570 °C using Eq. (1) gives directly the contribution due to organic units. Alternatively, one can calculate total percentage weight loss of the products in terms of hydroxyl units between temperature range of 150–570 °C using Eq. (1) and then subtract the actual hydroxyl units of un-reacted fullerenol (i.e. 28 in the present case) to get the contribution due to organic units. Thus, about 68, 70 and 51% weight loss between temperature ranges of 150–570 °C is observed from thermograms of 1a, 2a and 3a, respectively and structural degradation of fullerene above 570 °C plus char yield contribute 20, 25 and 42 weight% (Figs. 3–5 and Table 2).

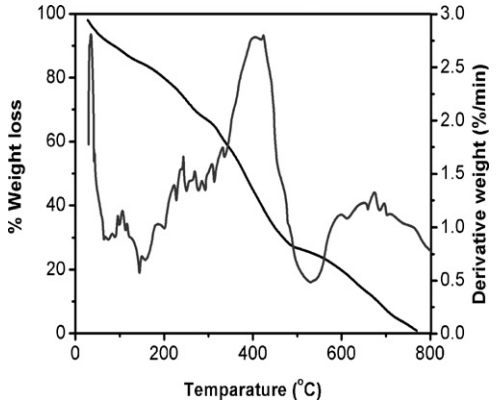

Fig. 3. TGA thermogram and first derivative curve of $(VE1a)_{28}$–C_{60} recorded at heating rate of 10 °C/min under N_2.

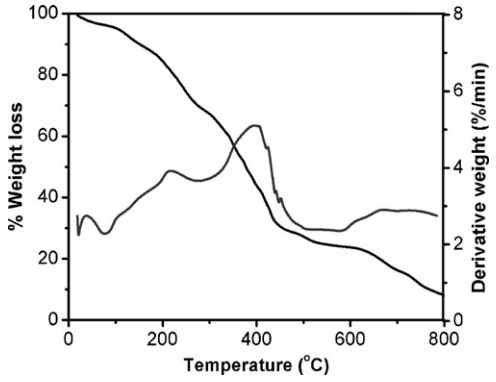

Fig. 4. TGA thermogram and first derivative curve of $(VE2a)_{28}$–C_{60} recorded at heating rate of 10 °C/min under N_2.

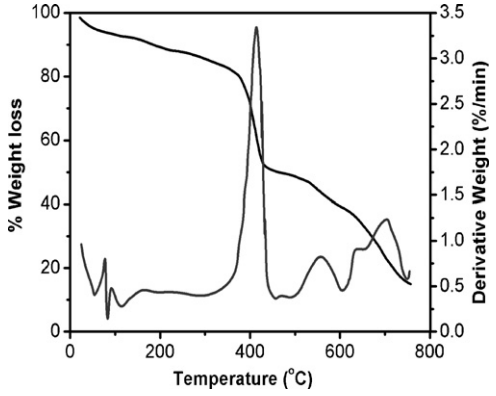

Fig. 5. TGA thermogram and first derivative curve of $(VE3a)_{28}$–C_{60} recorded at heating rate of 10 °C/min under N_2.

Table 2
Calculation of number of addends per fullerene on the basis of TGA technique reported earlier [47].

Code	% Weight loss			M	$n=(720/y\times x/M)$
	25–150 °C	150–570 °C (x)	>570 °C (y)		
Fol	13	52	35	17	28
1a	12	68	20	106	23
2a	5	70	25	93	21
3a	7	51	42	155	6
2b	7	75	18	93	32

Table 3
Accurate calculation of number of addends per fullerene for hemi-ortho esters (1a–3a and 2b) by modified method on the basis of TGA results.

Code	% Weight loss (temperature range°C)				
	Initial loss due to volatiles	x	y	M	$n=(720/y\times x/M)$
Fol	13(25–150)	52(150–570)	35(>570)	17	28
1a	7(25–110)	75(110–580)	18(>580)	106	28
2a	5(25–130)	74(130–660)	21(>660)	93	27
3a	5(25–130)	83(130–750)	12(>750)	155	27
2b	7(25–110)	75(110–580)	18(>580)	93	32

2.3.4. Direct calculation of organic units

For example, in case of (1a), unit mass of each vinyl ethanoate hemi-ortho ester (M) = 106 (molecular weight of vinyl ethanoate = 89 plus hydroxyl unit = 17). Then number of vinyl ethanoate hemi-ortho ester units attached per fullerene can be estimated as follows:

Percent weight loss in the temperature range 150–570 °C = 68.
Percent weight loss above 570 °C temperature plus char residue = 20.
Then, number of hemi-ortho ester units per fullerene = $(720/20)\times(68/106)\approx 23$.

2.3.5. Alternative hydroxyl groups equivalent method

Total number of hydroxyl groups equivalent per fullerene = $(720/20)\times(68/17)\approx 144$. There are about 28 –OH groups in unreacted fullerenol, then contribution of hemi-ortho ester units = 144 – 28 = 116 hydroxyl groups. Since molecular weight of one vinyl ethanoate unit is 89, then hydroxyl group equivalent for each vinyl ethanoate unit is equal to 5 ($89/17\approx 5$). Then number of vinyl ethanoate units attached per fullerene = 116/5 = 23.2–23 (since molecule cannot be fractioned). In a similar manner, number of hemi-ortho ester units attached per fullerene in other cases is also calculated (Table 2).

2.3.6. Modification of existing method

From Table 2, it is clear that number of addends calculated on the basis of mass loss shows dramatically low value for 3a due to incomplete removal of addends within 570 °C and also in other cases, calculated value is in slightly lower side due to overlapping of thermal events.

Therefore a little stringent approximation is made while applying this technique in present cases in order to get more accurate results [47]. First, it is assumed that there should not be any overlapping of thermal events at particular temperature zone under consideration. This means that thermo-gravimetric contribution comes from single thermal event only. This approximation clearly suggests that it is difficult to achieve universal temperature zone for all the system and it depends on the nature of addends. Secondly it is also assumed that particular thermal event must be completed within specified temperature zone and there will be no extension of temperature range for that particular thermal event. Overlapping thermal events give erroneous result. Based on these two assumptions, temperature zones are re-defined for each derivatives and x and y values are accurately calculated to get the exact mass loss. Modified temperature zone gives more precise values for x and y and hence the calculated number of addends in each case gives very close to theoretical values (Table 3).

2.4. Thermal analysis

TGA thermogram and the first derivative TGA trace of hemi-ortho ester derivatives and their comparison with unreacted

Table 4
Summary of degradation pattern for products (1a–3a and 2b) on the basis of TGA results between temperature ranges of 150 and 570 °C.

Code	Degradation (% weight loss)	Crest temperature (°C)
Fol	35	214.5
1a	61.66	250, 418
2a	44.56	248, 408.5
3a	43.16	516.2
2b	75	221.3, 414.9

fullerenol reveal several interesting observations not only to ascertain the chemical attachment of vinyl ester units onto the fullerene core but also to predict their thermo-chemical behavior. Typical TGA thermogram of fullerenol and hemi-ortho esters recorded at heating rate of 10 °C/min in N_2 atmosphere are presented in Figs. 3–5 and thermal data are summarized in Table 4. In first instant, all the boundary condition of earlier reported method [47] is applied to understand the efficacy of this model. Initial weight loss in all samples is assumed to be due to the removal of low boiling units inherently present in the samples. Typical characteristic thermal features that distinguish chemically modified fullerenol from pristine fullerenol are presented below: (i) removal of hemi-ketal hydroxyl groups occurring at higher temperature compared to OH group(s) of unreacted fullerenol. (ii) An additional degradation step (first derivative TGA) appears at higher temperature (410 °C or above) for all the samples which is absent in unreacted fullerenol. (iii) Percentage weight loss due to addends in the temperature range 150–570 °C is much higher in hemi-ortho esters compared to unreacted fullerenol and (iv) number of addends calculated on the basis of percentage weight loss in fullerenol (hydroxyl groups) and in products (addend units) are marginally comparable to each other except 3a [47]. Above observations provide information about the chemical attachment of vinyl ester units onto fullerene core. Hemi-ketal hydroxyl groups need higher temperature for de-hydroxylation (230–250 °C) compared to free hydroxyl groups in pristine fullerenol (crest temperature ~214 °C) owing to better encapsulation of OH-group through bulky vinyl ester groups. Additional degradation step at ~410 °C is solely because of vinyl ester units attached to fullerenol. Mass units of attached vinyl ester are much higher compared to hydroxyl groups and higher mass loss in the temperature range of 150–570 °C, therefore, nicely justifies the chemical attachment of vinyl esters units. Calculated average number of addended units in fullerenol and functionalized fullerenol validate this observation [47].

Presence of phenyl group in vinyl benzoate imparts better thermal stability in 3a. It is attributed that degradation of phenyl group occurs above 570 °C and experimental mass loss value recorded between temperature ranges of 150 and 570 °C is significantly low compared to theoretically calculated value. Consequently the number of addends calculated on the basis of mass loss shows drastically low value compared to other cases. Similarly, slightly lower value in other cases is attributed to overlapping of thermal events below 150 °C. It is believed that degradation of addends have started much below 150 °C and completed above 570 °C. Therefore the temperature zone of earlier approach has been modified to get precise values of x and y. Table 3 provides correct values of number of addends estimated under present condition.

TGA thermograms of $(VE1a)_{28}–C_{60}$ (Fig. 3) and $(VE2a)_{28}–C_{60}$ (Fig. 4) follow similar pattern, showing monotonic weight loss up to 350 °C followed by a sharp degradation step between the temperature range 350–450 °C. First derivative TGA traces of $(VE2a)_{28}–C_{60}$ shows multi-step de-hydroxylation between temperature range of 150 and 300 °C for the removal of hemi-ketal hydroxyl groups (crest temperature 248 °C) and vinyl acetate units between the temperature range of 300 and 570 °C (crest temperature 408 °C). Slightly better thermal stability with longer alkyl group is evident

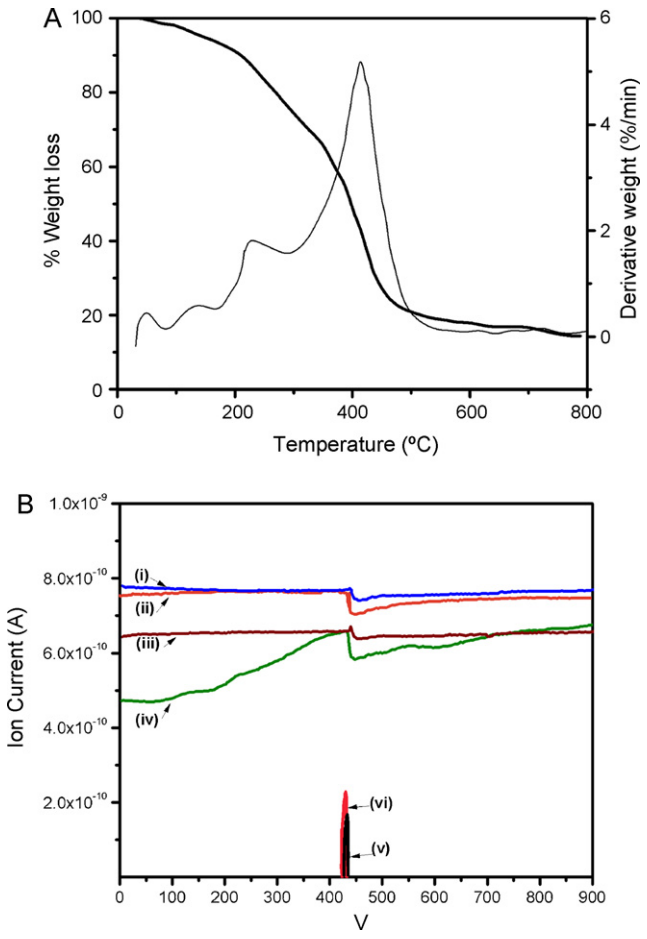

Fig. 6. (A) TGA thermogram of $(VE2b)_{28}–C_{60}$ recorded under N_2 atm. at a heating rate of 10 °C/min. (B) TG-MS of $(VE2b)_{28}–C_{60}$ recorded under N_2 atm. at a heating rate of 10 °C/min showing the evolution of (i) ethylene (28), (ii) water (18), (iii) hydroxyl (17), (iv) vinyl alcohol/acetaldehyde (44), (v) ethane (30) and (vi) butane (58) molecules.

from the higher crest temperature for vinyl propionate–fullerenol adduct $(VE1a)_{28}–C_{60}$ [crest temperature 418 °C]. Higher thermal stability due to incorporation of aromatic moiety is observed in TGA and first derivative TGA trace of vinyl benzoate derivative (Fig. 5) of fullerenol [$(VE3a)_{28}–C_{60}$]. TGA thermogram shows nearly plateau-region up to about 400 °C with a percent weight loss ~15% [compared to ~60% in $(VE1a)_{28}–C_{60}$ and $(VE2a)_{28}–C_{60}$] followed by sharp degradation step between the temperature range 400 and 550 °C with a percent weight loss of ~30%. Corresponding 1st derivative records a clear and sharp degradation step having crest temperature 516.20 °C. Char yield of material is also higher (~20%) than other products. TGA and first derivative TGA thermogram show better thermal stability of heterogeneous phase product $(VE2b)_{28}–C_{60}$ (Fig. 6A) compared to homogeneous phase product. Weight loss of ~20% between 150 and 300 °C and ~55% between 300 and 570 °C is observed. Char yield of the material is 23%. There are ~32 addends calculated on the basis of mass loss which is substantially higher compared to unreacted fullerenol (Tables 2 and 3). It is attributed that higher value is due to the release of entrapped TBAH and its contribution during thermal measurement. TG-MS for $(VE2b)_{28}–C_{60}$ is recorded under inert atmosphere at a heating rate of 10 °C/min. Desorption of physically absorbed water molecules at temperature below 150 °C is detected (Fig. 6B). Presence of entrapped tetra butyl ammonium hydroxide impurity in the product is also detected. Thermal evolution of butyl chain (mass value 57) is observed at ~425 °C along with other molecules like ethy-

lene (from vinyl group, mass 27) and vinyl alcohol/acetaldehyde (HO–CH=CH_2/CH_3CHO, mass 44). Calculated higher number of addends (on the basis of experimental mass value) compared to unreacted fullerenol (~28 OH-groups) nicely justifies TG-MS findings for the existence of small TBAH impurity in 2b. Interestingly, this small TBAH impurity induces a significant doping effect on photophysical properties of the products also [55].

3. Conclusions

Above results provide an opportunity to explore the potency of simple thermo gravimetric analysis to evaluate average number of addends and various thermal characteristic properties of new class of fullerene dyad materials. Presence of substituent in addends contributes significantly to the overall stability of the dyads and made an interesting effect during the calculation of number of addends attached on fullerene. Necessary correction to get exact values of *x* and *y* thus provides correct number of addends in vinyl hemi-ortho ester dyads. Thermal analysis also shows an effect of entrapped TBAH while calculating number of addends in two phase system. Selectivity of fullerenol towards carbonyl group in alkaline medium contributed significantly in designing simple and viable synthesis route for the preparation of stable hemi-ortho esters. Geometrical orientation and large number of flexibly ether linked vinylic double bonds in close proximity induces delocalization of π-electrons and interaction between these delocalized vinylic electrons and fullerene core, which is strongly reflected in appearance of structured bands in absorption spectrum[21]. Study of photophysical property of these materials reveal that these double bonds behave more close to π-conjugated system than free isolated double bonds [21]. These free π-bonds provide an opportunity to play on the conventional chemistry to develop new materials.

4. Experimental

4.1. Materials

[60]Fullerene (C_{60}) (MER Co., purity >99.5%), vinyl esters (vinyl acetate, vinyl propionate and vinyl benzoate), sodium hydroxide, tetra butyl ammonium hydroxide (TBAH) have been purchased from Acros and used as received. Methanol and other solvents (spectroscopy grade E Merck) are purified and dried (as per standard procedure) before use.

4.2. Single-phase synthesis

4.2.1. General method

The methanolic solution of vinyl ester (1–3, 10 eq. per hydroxyl group) is added slowly to an ice cooled mix alkaline aqueous solution of fullerenol (0.04 mM) and conc. NaOH solution (1 g in 2 mL water) under inert atmosphere. Temperature is slowly raised to r.t. and stirred for 24 h under inert atmosphere. The orange-red solid products are extracted with dichloromethane and purified by column chromatography.

4.2.1.1. $(VE1a)_{28}$–C_{60}. FTIR (KBr, cm^{-1}) 3426 (n, O–H), 3090 (n, =C–H), 2972, 2931 (n, C–H), 1675 (n, C=C), 1450, 1375, 1312 (d, C–H), 1080 (d, ether C–O), 950 (d, =CH_2), 872 (out of plane CH=C bending). ^1H and ^{13}C NMR ($CDCl_3$, d): 1.29 (CH_3), 3.2 (CH_2), 5.74 (=CH_2–) and 6.68 (–*CH*=) and 21.11 (*C*H_3), 55.92 (–*C*H_2–), 193 [–O–*C*(OH)–O–] and the broad hump between 120 and 140 ppm for the fullerene and vinylic carbons. ESI-MS (*m*/*z*, %, fragment) 3980 (25, M+, C_{60} + 28 units + OH), 3880 (100, C_{60} + 27 units), 3810 (50, C_{60} + 26 units + OH + MeOH), 3640 (50, C_{60} + 24 units + OH + 3MeOH), 3545 (25, C_{60} + 24 units + OH), 3410 (15, C_{60} + 23 units), 3210 (45, C_{60} + 21 units + 2OH), 3145 (5, C_{60} + 21 units + 2OH), 2955 (60, C_{60} + 18 units + 4MeOH), 2570 (58, C_{60} + 15 units + 3MeOH), 2475 (32, C_{60} + 15 units), 2190 (55, C_{60} + 12 units + 2OH + MeOH), 2125 (10, C_{60} + 12 units), 2007 (5, C_{60} + 11 units), 1088 (12, C_{60} + 3 units + OH), 1006 (95, C_{60} + 2 units + 3OH). UV–vis (labs, Methanol, nm) 236, 286.

4.2.1.2. $(VE2a)_{28}$–C_{60}. FTIR (KBr, cm^{-1}) 3428 (n, O–H), 3090 (n, =C–H), 2973, 2925 (n, C–H), 1678 (n, C=C), 1452, 1376 (d, C–H), 1086 (d, ether C–O), 754 (out of plane, C–H bending). ^1H and ^{13}C NMR ($CDCl_3$, d): 1.2 (3H, s, CH_3), 5.7 (=CH2), and 6.5 (–O–CH=) and δ 15–20 (*C*H_3), 55–70 (sp^3 hybridized carbons of fullerene), 100–110 (=*C*H2), 143 ppm (–O–*C*H=) and 193 [quaternary carbon [–*C*(–O–)$_3$]. ESI-MS (*m*/*z*, %, fragment) 3490 (10, M+, C_{60} + 27 units + OH – vinyl unit), 3424 (50, C_{60} + 25 units + 3OH + NaOH), 3352 (5, C_{60} + 25 units + OH + NaOH), 3289 (30, C_{60} + 24 units + 3MeOH), 3171(45, C_{60} + 23 units + 3OH + 3MeOH), 3043 (48, C_{60} + 22 units + 2OH + Na), 2980 (20, C_{60} + 21 units + 2OH + 2MeOH), 2819 (100, C_{60} + 20 units + OH + Na), 2768 (5, C_{60} + 19 units + 4OH + Na), 2663 (35, C_{60} + 18 units + 4OH + Na), 2584 (30, C_{60} + 17 units + 4OH + Na), 2466 (52, C_{60} + 16 units + 4OH + MeOH), 2350 (20, C_{60} + 16 units – OH), 2282 (40, C_{60} + 15 units + OH), 2216 (12, C_{60} + 14 units + 3OH), 2114 (12, C_{60} + 13 units + 17 2OH + Na), 2038 (50, C_{60} + 12 units + 5OH), 1991 (5, C_{60} + 12 units + 2OH), 1916 (30, C_{60} + 11 units + 2MeOH), 978 (5, C_{60} + 2 units + 3OH). UV–vis (labs, methanol, nm) 276, 327. PL (λ_{em}) (solid, nm) 635, 673.

4.2.1.3. $(VE3a)_{28}$–C_{60}. FTIR (KBr, cm^{-1}) 3422 (n, O–H), 3090 (n, =C–H), 3062 (n, aromatic =C–H), 1598 (n, C=C), 1552, 1412 (n, aromatic C=C), 1067 (d, ether C–O, asy), 1028 (d, ether C–O, sy), 950 (d, =CH2), 844 (d, CH=), 710 (in plane aromatic =C–H bending), 680 (out of plane aromatic C–H bending). ^1H and ^{13}C NMR ($CDCl_3$, d): 7.45–7.56 (aromatic) 5.7 and 6.5 (vinylic) and 131–139 (sp^2 hybridized carbons), 176 (for substituted benzene carbon) and 178 [–O–*C*(OH)–O–] ppm. ESI MS (*m*/*z*, %, fragment) 4485 (10, M+, C_{60} + 23 units – OH), 4425 (50, C_{60} + 23 units – 4OH – vinyl), 4385 (5, C_{60} + 22 units + MeOH), 4370 (30, C_{60} + 22 units+ H_2O), 4315 (45, C_{60} + 22 units–2OH), 4205 (48, C_{60} + 21 units + H_2O), 4155 (20, C_{60} + 20 units + 8OH), 4100 (100, 4155-2 vinyl), 4090 (5, C_{60} + 20 units + 4OH), 4050 (35, C_{60} + 20 units + 2OH), 3872 (30, C_{60} + 19 units + OH), 3810 (52, C_{60} + 18 units + 7OH), 3720 (20, C_{60} + 18 units + 2OH), 3620 (40, C_{60} + 17 units + 2OH + MeOH), 3530 (12, C_{60} + 16 units + 10OH), 3460 (12, C_{60} + 16 units + 6OH), 3390 (50, C_{60} + 16 units + 2OH), 3330 (5, C_{60} + 15 units + 8OH), 3250 (30, C_{60} + 15 units + 3OH), 3195 (5, C_{60} + 15 units), 3090 (12, C_{60} + 14 units + 2MeOH), 3010 (50, C_{60} + 14 units–OH), 2985 (5, C_{60} + 13 units + 7OH), 2880 (30, C_{60} + 13 units + OH), 2770 (5, C_{60} + 12 units + 4OH), 2755 (12, C_{60} + 12 units + 3OH), 2655 (50, C_{60} + 11 units + 7OH). UV–vis (labs, methanol, nm) 204, 240, 262, 280.

5. Characterization techniques

Fourier transformed infra-red (FT-IR) spectra are recorded on a Nicolet Magna IR 750 Spectrometer, using potassium bromide pellets. The Ultra violet–visible (UV–Vis) spectra of the products are recorded on a Varian-CARY 500 UV-VIS-NIR spectrophotometer in solution. ^1H and ^{13}C nuclear magnetic resonance (NMR) spectra are recorded on Brucker Av 400 spectrometer operating at frequency of 400 MHz in different deuterated solvents. Electrospray mass spectra (ESI-MS) are recorded on a MICROMASS QUATTRO II triple quadrupole mass spectrometer. Methanolic solution of the samples was introduced into the ESI source through a syringe pump at the rate of 5 μL/min. The ESI capillary is set at 3.5 kV and the cone voltage is 40 V. The spectra are collected in 6 s scans and the

print outs are averaged spectra of 6–8 such scans. Thermal properties are measured using a Hi-Res TGA 2950 Thermogravimetric Analyzer (TA Instruments) attached to a Thermal Analyst 2100 (Du Pont Instruments) thermal analyzer, at a heating rate of 10 °C/min under N_2 atmosphere. The enthalpy change associated with the dehydroxylation of fullerene derivatives was determined using differential scanning calorimetry (DSC) at a heating rate of 10 °C/min upto 500 °C using a TA Instrument Inc. Thermal Analyst System model 2100 equipped with a model 2910 DSC cell. The sample compartment is purged with dry nitrogen at 50 mL/min. The surface topographical structures of the samples are studied by JEOL, JSM-840 scanning electron microscope (SEM). The samples are spread on a double adhesive tape supported on a brass substance. After mounting the sample are coated with gold in plasma sputter unit and then analyzed by SEM at 5 kV. Electron spectroscopy for chemical analysis (ESCA) is obtained by X-ray photoelectron spectrometer equipped with a monochromatic X-ray source. ESCA analysis is performed at a nominal photoelectron take off angle of 45° and the depth of analysis for these samples is 100 Å. The relative atomic% of each element at the surface is estimated from the peak areas using atomic sensitivity factors specified for the spectrometer. A BAS Epsilon-EC-Ver 1.40.67 Cyclic Voltammeter/Autolab are used for cyclic voltammetric analysis having platinum disc working electrode, a platinum wire counter electrode and pseudo Ag/AgCl reference electrode in a single compartment. The measurements are carried out at the scan rate of 100 mV/s. The reversible oxidation signal of Ferrocene/Ferrocenium (Fc/Fc^+) is used as the internal reference. Tetra butyl ammonium perchlorate as the supporting electrolyte is used after purification and drying according to standard procedure.

Appendix A. Supplementary data

Supplementary data associated with this article can be found, in the online version, at doi:10.1016/j.tca.2010.11.012.

References

[1] H. Imahori, Y. Mori, Y. Matano, J. Photochem. Photobiol. C 4 (2003) 51–83.
[2] J.F. Nierengarten, Top. Curr. Chem. 228 (2003) 87–110.
[3] D.M. Guldi, Pure Appl. Chem. 75 (2003) 1069–1075.
[4] M.E. El-Khouly, O. Ito, F. D'Souza, J. Photochem. Photobiol. C 5 (2004) 79–104.
[5] D.M. Guldi, M. Prato, Chem. Commun. (2004) 2517–2525.
[6] D.M. Guldi, J. Phys. Chem. B 109 (2005) 11432–11441.
[7] J.L. Segura, F. Giacalone, R. Gómez, N. Martın, D.M. Guldi, C. Luo, A. Swartz, I. Riedel, D. Chirvase, J. Parisi, V. Dyakonov, N.S. Sariciftci, F. Padinger, Mater. Sci. Eng. C 25 (2005) 835–842.
[8] G.N. Manuel, S. Sepas, R. Alain, M. Patrick, N. Jean-Francois, New J. Chem. 26 (2002) 1584–1589.
[9] W.-B. Zhang, Y. Tu, R. Ranjan, R.M. Van Horn, S. Leng, J. Wang, M.J. Polce, C. Wesdemiotis, R.P. Quirk, G.R. Newkome, S.Z.D. Cheng, Macromolecules 41 (2008) 515–517.
[10] Y. Matsuo, E. Nakamura, Chem. Rev. 108 (2008) 3016–3028.
[11] N. Martín, L. Sánchez, B. Illescas, I. Pérez, Chem. Rev. 98 (1998) 2527–2548.
[12] J.-F. Nierengartenm, J.-F. Nicoud, L. Ouali, V. Krasnikov, G. Hadziioannou, Chem. Commun. (1999) 617–618.
[13] Q. Xie, E. Perez-Cordero, L. Echegoyen, J. Am. Chem. Soc. 114 (1992) 3978–3980.
[14] A. Hirsch, Fullerenes and Related Structures, Topics in Current Chemistry, vol. 199, Springer, Berlin, 1999.
[15] S. Fukuzumi, K. Ohkubo, H. Imahori, D.M. Guldi, Chem. Eur. J. 9 (2003) 1585–1593.
[16] H. Mohan, D.K. Palit, J.P. Mittal, L.Y. Chiang, K.D. Asmus, D.M. Guldi, J. Chem. Soc. Faraday Trans. 94 (1998) 359–363.
[17] D.K. Palit, H. Mohan, J.P. Mittal, J. Phys. Chem. A 102 (1998) 4456–4461.
[18] D.K. Palit, H. Mohan, P.R. Birkett, J.P. Mittal, J. Phys. Chem. A 101 (1997) 5418–5422.
[19] R.V. Bensasson, T.J. Hill, E.J. Land, S. Leach, D.J. McGarvey, T.G. Truscott, J. Ebenhoch, M. Gerst, C. Ruchart, Chem. Phys. 215 (1997) 111–123.
[20] K.M. Kadish, X. Gao, C.E. Van, T. Hirasaka, T. Suenobu, S. Fukuzumi, J. Phys. Chem. 102 (1998) 3898–3906.
[21] R. Singh, T.H. Goswami, Synth. Met. 157 (2007) 951–955.
[22] Y.M. Li, K. Hinokuma, Solid States Ionics 150 (2002) 309–315.
[23] K. Hinokuma, M. Ata, Chem. Phys. Lett. 341 (2001) 442–446.
[24] S. Campidelli, J. Lenoble, J. Barbera, F. Paolucci, M. Marcaccio, D. Paolucci, R. Deschenaux, Macromolecules 38 (2005) 7915–7925.
[25] W.-S. Li, K.S. Kim, D.-L. Jiang, H. Tanaka, T. Kawai, J.H. Kwon, D. Kim, T. Aida, J. Am. Chem. Soc. 128 (2006) 10527–10532.
[26] A.W. Jansen, S.R. Wilson, D.J. Schuster, Bioorg. Med. Chem. 4 (1996) 767–779.
[27] T.D. Ros, M. Prato, Chem. Commun. (1999) 663–669.
[28] L.J. Wilson, Medical applications of fullerenes and metallofullerenes, Electrochem. Soc. Interface (1999) 24–28.
[29] S. Bosi, T. Da Ros, G. Spalluto, M. Prato, Eur. J. Med. Chem. 38 (2003) 913–923.
[30] N. Tagmatarchis, H. Shinohara, Med. Chem. 1 (2001) 339–348.
[31] L.Y. Chiang, F.J. Lu, J.T. Lin, in: P. Bernier, D.S. Bethune, L.Y. Chiang, T.W. Ebbesen, R.M. Matzger, J.W. Mintmire (Eds.), Science and Technology of Fullerene Materials, Materials Research Society, Pittsburgh, 1995, p. p327.
[32] B.C. Wang, C.Y. Cheng, Mol. Struct. (THEOCHEM) 179 (1997) 391.
[33] Y.S. Chun, H.G. Li, R.W. Chun, P. Xin, H. Hong, Carbon 44 (2006) 496–500.
[34] R.D. Bolskar, A.F. Benedetto, L.O. Husebo, R.E. Price, E.F. Jackson, S. Wallace, J. Am. Chem Soc. 125 (2003) 5471–5478.
[35] B. Sitharaman, R.D. Bolskar, I. Rusakova, L.J. Wilson, Nano Lett. 4 (2004) 2373–2378.
[36] M. Mikawa, H. Kato, M. Okumura, M. Narazaki, Y. Kanazawa, N. Miwa, Bioconjugate Chem. 12 (2001) 510–514.
[37] H. Kato, Y. Kanazawa, M. Okumura, A. Taninaka, T. Yokawa, H. Shinohara, J. Am. Chem. Soc. 125 (2003) 4391–4397.
[38] I. Lamparth, C.M. Mossmer, A. Hirsch, Angew. Chem. Int. Ed. Eng. 34 (1995) 1607–1609.
[39] J. Shinar, Z.V. Vardeny, Z.H. Kafafi, Optical and Electronic Properties of Fullerene and Fullerene-Based Materials, Marcel Dekker Publications, New York, 2000, pp. 43–81.
[40] J. Li, A. Takeuchi, M. Ozawa, X. Li, K. Saigo, K. Kitazawa, J. Chem. Soc. Chem. Commun. (1993) 1784–1785.
[41] T.H. Goswami, R. Singh, Entitled recent development of fullerenol research, in: Carl N. Kramer (Ed.), Fullerene Research Advances, NOVA Science Publishers, NY, 2007, ISBN 1-60021-824-5, pp. 55–96 (Chapter 3). On reducing the of NaOH to 100 times (2 g in 200 mL), the same reaction can produce $C_{60}(OH)_{16-18}$, whereas reducing the amount of NaOH and time (0. 15 g NaOH in 10 mL water, 2 h), the reaction yields $C_{60}(OH)_{12-14}$.
[42] T.H. Goswami, B. Nandan, S. Alam, G.N. Mathur, Polymer 44 (2003) 3209–3214.
[43] T.H. Goswami, R. Singh, S. Alam, G.N. Mathur, Chem. Mater. 16 (2004) 2442–2448.
[44] R. Singh, T.H. Goswami, J. Phys. Org. Chem. 21 (2008) 225–236.
[45] L.Y. Chiang, L.Y. Wang, S.M. Tseng, J.S. Wu, K.H. Hseih, J. Chem. Soc. Chem. Commun. (1994) 2675–2676.
[46] R. Singh, T.H. Goswami, J. Organomet. Chem. 693 (2008) 2021–2032.
[47] T.H. Goswami, R. Singh, S. Alam, G.N. Mathur, Thermochim. Acta 419 (2004) 97–104.
[48] G.A. Rogers, T.C. Bruice, J. Am. Chem. Soc. 96 (1974) 2481–2488.
[49] F.F. Khouri, M.K. Kaloustain, J. Am. Chem. Soc. 108 (1986) 6683–6695.
[50] B. Capon, M.I. Dosunmu, M. Sanchez, Adv. Phys. Org. Chem. 21 (1985) 37–98.
[51] R.A. McClellend, L.J. Santry, Acc. Chem. Res. 16 (1983) 394–399.
[52] B.A. Capon, K. Ghosh, D.M.A. Grieve, Acc. Chem. Res. 14 (1981) 306–312.
[53] A.M. Lobo, M.M. Marques, S. Prabhakar, H. Rzepa, J. Chem. Soc. Chem. Commun. (1985) 1113–1115.
[54] L.O. Husebo, B. Sitharaman, K. Furukawa, T. Kato, L.J. Wilson, J. Am. Chem. Soc. 126 (2004) 12055–12064.
[55] R. Singh, T.H. Goswami, Photophysical and optical limiting properties of multifunctional hemi-ortho ester derivative of fullerenol: effects of TBAH doping, fullerenol concentration and solvent polarity (2010, communicated).